Proceedings of the 2006 IEEE International Conference on Robotics and Automation
Orlando, Florida - May 2006

Accurate Force Reflection for Kinematically Dissimilar Bilateral Teleoperation Systems Using Instantaneous Restriction Space

Keehoon Kim† Wan Kyun Chung† Il Hong Suh‡
†*Robotics and Bio-Mechatronics Lab., Pohang Univ. of Sci. and Tech, POSTECH, KOREA*
‡*Graduate School of Information and Communications Hanyang University, KOREA*
E-mail: †{khk,wkchung}@postech.ac.kr, ‡ihsuh@hanyang.ac.kr

***Abstract*— This paper proposes restriction space projection (RSP) method to generate accurate direction of force reflection when a bilateral teleoperation system (BTS) is kinematically dissimilar. Through examples, it is shown that the previous force reflection methods are not applicable to the kinematically dissimilar BTSs. Two kinds of RSP methods using a novel concept, instantaneous restriction space (IRS), are implemented for impedance and admittance type of BTSs. Especially, new developed obstacle avoidance algorithm using the redundancy of the slave manipulator makes the RSP method applicable to all kinds of kinematically dissimilar BTSs. Experiments verify that the RSP method is powerful to describe the restriction space at the slave side without force sensors.**

I. Introduction

Accurateness of force reflection is one of criteria to measure performance of bilateral teleoperation systems (BTSs). Although, for the last decades, researchers have made efforts to increase the presence of force reflection, the frameworks for force reflection have little changed from position-position (p-p) architecture, position-force (p-f) architecture, and their combinations such as general four-channel architecture (Table I).

It is known that the previous conventional architectures have limitation to apply to kinematically dissimilar BTSs. Kim introduced an example to show that it makes serious problem if only force reflection under p-f architecture is used without p-p architecture at unstructured environment [13]. Therefore, p-f architecture should be used with p-p architecture by the way of precaution against collision of unexpected obstacle when force sensors can not detect. Kim also showed that the conventional p-p architecture has limitation to generate accurate direction of force reflection for kinematically dissimilar multi DOF BTSs.

The kinematic dissimilarity is defined in TABLE II when Jacobian of the master device, $\boldsymbol{J}_m : \dot{\boldsymbol{q}}_m \in \mathbb{R}^m \rightarrow \dot{\boldsymbol{x}}_m \in \mathbb{R}^r$, and Jacobian of the slave manipulator, $\boldsymbol{J}_s : \dot{\boldsymbol{q}}_s \in \mathbb{R}^n \rightarrow \dot{\boldsymbol{x}}_s \in \mathbb{R}^r$, where $\boldsymbol{q}_m$ and $\boldsymbol{q}_s$ are the joint angles of the master and slave manipulator in the joint spaces, $\mathbb{R}^m$ and $\mathbb{R}^n$, respectively. $\boldsymbol{x}_m$ and $\boldsymbol{x}_s$ are the pose of the master and slave manipulator in the task space $\mathbb{R}^r$. Note that it is different from geometric similarity. For example, if the length scale ratio of a master device is the same with that of a slave manipulator, it is geometrically similar but not kinematically similar.

TABLE II
Definition of the kinematic dissimilarity

case 1	$\boldsymbol{J}_m = \boldsymbol{J}_s$ Kinematically similar haptic interface
case 2	$\boldsymbol{J}_m \neq \boldsymbol{J}_s$, $m = n$ Kinematically dissimilar haptic interface with the same DOF
case 3	$\boldsymbol{J}_m \neq \boldsymbol{J}_s$, $m > n$ Kinematically dissimilar haptic interface with insufficient DOF at the slave side
case 4	$\boldsymbol{J}_m \neq \boldsymbol{J}_s$, $m < n$ Kinematically dissimilar haptic interface with redundance at the slave side

TABLE III
Application Ranges of Force Reflection Methods
(O : applicable, X : not applicable)

	case 1	case 2,3	case 4
conventional p-p	O	X	X
Kim [13]	O	O	X
proposed framework	O	O	O

The kinematic dissimilarity can be classified into 4 cases as shown in TABLE II. The conventional p-p architecture is applicable only to single DOF or kinematically similar BTSs. Kim's framework can be applied to case 1-3. However, when the slave manipulator has redundancy compared to the master device, his method cannot be used anymore. The proposed method in this paper covers every case of kinematic dissimilarity as shown in TABLE III.

In this paper, we focus on the force reflection covering all 4 cases without force sensor since it is burdensome to distribute enough force sensors to detect every possible collision in practical applications. In section II, the motivation of this paper is explained. Section III introduces instantaneous restriction space and implementation method of the proposed force reflection using IRS. A case study proves that the proposed method can solve the limitation of the conventional force reflection framework in section III. Section IV explains how to create instantaneous restriction space for the case 4 in TABLE II. Experimental results are discussed in section V and followed

TABLE I
ARCHITECTURES OF BTSS & HAPTIC INTERFACES IN LITERATURE

Author(s)	Architecture	Feature
[1] Hannaford (1989)	p-f	Two-port network design framework
[2] Anderson and Spong (1989)	p-f	Passivity analysis using scattering matrix
[3] Niemeyer and Slotine (1991)	p-f	Wave variable for time delayed interface
[4] Lawrence (1993)	p-p & p-f	Necessity of four-channel for high levels of transparency
[5] Yokokohji and Yoshikawa (1994)	p-f	Maneuverability evaluation
[6] Colgate and Brown (1994)	p-f	Z-width, achievable impedance range
[7] Oboe and Fiorini (1998)	p-p	Adaptive teleoperation
[8] Adams and Hannaford (1999)	p-f, f-p	Z-width evaluation for impedance and admittance interface
[9] Hannaford and Ryu (2002)	p-f	Time domain passivity
[10] Zaad and Salcudeann (2002)	p-f	Local force feedback for transparency in time delayed system
[11] Cavusoglu *et al.* (2002)	p-p & p-f	Comparison of p-p and p-f for fidelity
[12] Imaida *et al.* (2004)	p-p	Teleoperation under long time-delay condition

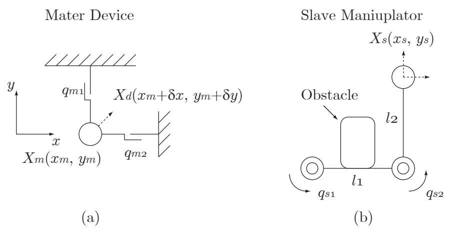

Fig. 1. Constrained condition by an obstacle which is not detectable with force sensor

by conclusion in section VI.

II. LIMITATION OF PREVIOUS FORCE REFLECTION METHOD

This section explains the limitation of a force reflection method using conventional architecture in kinematically dissimilar bilateral teleoperation systems (BTSs). Kim showed that, as described before, the conventional p-p architecture has limitation to reflect accurate direction of force for kinematically dissimilar multi DOF BTSs assuming that BTSs use joint space control as a local controller [13]. In this section, we introduce limitation of the conventional p-p architecture even when task space controller is used for a multi DOF BTS through an example.

Fig.1 shows a kinematically dissimilar 2-DOF BTS in which the first joint of the slave manipulator is constrained by an unexpected obstacle so that force sensors can not detect the obstacle. x_m and x_s are position of the master device and the slave manipulator, respectively. q_{m1} and q_{m2} are length of the first and the second translational joint of the master device. q_{s1} and q_{s2} are the first and the second revolute joint angle of the slave manipulator. l_1 and l_2 are length of the first and the second link of the slave manipulator. Initially, the master and the slave manipulator has the same position, i.e., $\boldsymbol{X}_m(0) = \boldsymbol{X}_s(0)$. When a human operator tries to move the master device with small variation from $\boldsymbol{X}_m$ to $\boldsymbol{X}_d$, the reflecting force is generated through position tracking controller, $\boldsymbol{K}_m$ as the following procedure.

1) A new desired position caused by the variation of a master device, $\boldsymbol{X}_d$, is transferred to a slave manipulator.
2) The local position tracking controller at the slave side generates control input to the slave manipulator.
3) The position of the slave manipulator, $\boldsymbol{X}_s$, does not converge to the desired position, $\boldsymbol{X}_d$, by the obstacle.
4) The actual position of the slave manipulator, $\boldsymbol{X}_s$, is transferred to the master device.
5) The master device reflects the force using the position error, $\boldsymbol{F}_R = \boldsymbol{K}_m(\boldsymbol{X}_s - \boldsymbol{X}_d)$.

The Jacobians of the 2-DOF master and slave manipulator can be expressed as follows.

$$\boldsymbol{J}_m = \frac{\partial \boldsymbol{x}_m}{\partial \boldsymbol{q}_m} = \begin{bmatrix} 1 & 0 \\ 0 & 1 \end{bmatrix} \in \mathcal{R}^{2\times 2} \text{and} \tag{1}$$

$$\begin{aligned} \boldsymbol{J}_s &= \frac{\partial \boldsymbol{x}_s}{\partial \boldsymbol{q}_s} \\ &= \begin{bmatrix} -l_1 S(q_{s1}) - l_2 S(q_{s1}+q_{s2}) & -l_2 S(q_{s1}+q_{s2}) \\ l_1 C(q_{s1}) + l_2 C(q_{s1}+q_{s2}) & l_2 C(q_{s1}+q_{s2}) \end{bmatrix} \\ &\in \mathcal{R}^{2\times 2}. \end{aligned} \tag{2}$$

Two kinds of control strategies, joint space control and task space control, are available. The following example shows the limitation of the conventional p-p architecture, i.e., wrong direction of force reflection, when task space control is used.

The kinematics of the slave manipulator can be represented as

$$\boldsymbol{X}_s(t) = \begin{bmatrix} x_s(t) \\ y_s(t) \end{bmatrix} = \begin{bmatrix} l_1 C(q_{s1}(t)) + l_2 C(q_{s1}(t)+q_{s2}(t)) \\ l_1 S(q_{s1}(t)) + l_2 S(q_{s1}(t)+q_{s2}(t)) \end{bmatrix}. \tag{3}$$

If the dynamics of the slave manipulator is assumed to have only inertia term in order to make the problem simple and plain, it can be represented as

$$\boldsymbol{\tau}_s(t) = \begin{bmatrix} \tau_{s1}(t) \\ \tau_{s2}(t) \end{bmatrix} = \begin{bmatrix} H_{11} & H_{12} \\ H_{21} & H_{22} \end{bmatrix} \begin{bmatrix} \ddot{q}_{s1}(t) \ddot{q}_{s2}(t) \end{bmatrix} + \begin{bmatrix} F_{e1}(t) \\ F_{e2}(t) \end{bmatrix}, \tag{4}$$

where $\boldsymbol{\tau}_s(t)$ control input generated by task space controller. $H_{ij}(i,j=1,2)$ are inertia terms of the slave manipulator. $F_i(i=1,2)$ are the external forces by exogenous inputs like interaction force between manipulator and obstacles.

If the task space controller is assumed as simple p-gain

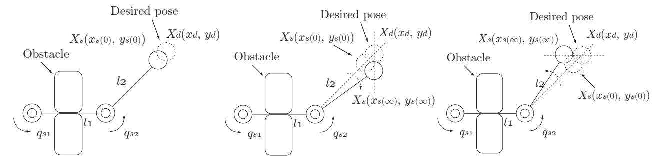

(a) (b) (c)

Fig. 2. (a) : Initial pose of the slave manipulator and desired pose, (b) : Equilibrium pose of the slave manipulator under task space control when $K_x \gg K_y$, (c) : Equilibrium pose of the slave manipulator under task space control when $K_x \ll K_y$.

controller as

$$\boldsymbol{\tau}_s(t) = \boldsymbol{J}_s^T \begin{bmatrix} K_x & 0 \\ 0 & K_y \end{bmatrix} \begin{bmatrix} e_1 \\ e_2 \end{bmatrix}, \tag{5}$$

where,

$$\begin{aligned} e_1 &= x_m(0) + \delta_x - l_1 C(q_{s1}(t)) - l_2 C(q_{s1}(t) + q_{s2}(t)) \text{ and} \\ e_2 &= y_m(0) + \delta_y - l_1 S(q_{s1}(t)) - l_2 S(q_{s1}(t) + q_{s2}(t)). \end{aligned}$$

If only the motion of the first joint is constrained by the obstacle, then $F_{e2} = 0$ and $\dot{q}_{s1}(t) = 0$. From Eq.(4) and Eq.(5), the dynamics of the slave manipulator can be derived as

$$\begin{aligned} H_{22}\ddot{q}_{s2}(t) &= K_x\{-l_2 S(q_{s1}(t) + q_{s2}(t)\} \\ &\quad \{x_m(0) + \delta_x - l_1 C(q_{s1}(t)) - l_2 C(q_{s1}(t) \\ &\quad + q_{s2}(t))\} + K_y\{l_2 C(q_{s1}(t) + q_{s2}(t))\} \\ &\quad \{y_m(0) + \delta_y - l_1 S(q_{s1}(t)) - l_2 S(q_{s1}(t) \\ &\quad + q_{s2}(t))\} \end{aligned} \tag{6}$$

If $l_1 = l_2 = 1$, $q_{s1}(0) = 0$, $q_{s2}(0) = 45°$, $x_m(0) = x_s(0)$, $y_m(0) = y_s(0)$, and $\delta_x = \delta_y$ as shown in Fig.2(a), then Eq.(6) can be simplified as

$$q_{s1}(t) = 0 \tag{7}$$

$$\begin{aligned} H_{22}\ddot{q}_{s2}(t) &= K_x\{-S(q_{s2}(t))\}\{x_s(0) + \delta_x - 1 - C(q_{s2}(t))\} \\ &+ K_y\{C(q_{s2}(t)\}\{y_s(0) + \delta_y - S(q_{s2}(t))\} \end{aligned} \tag{8}$$

From Eq.(8), if $K_x \gg K_y$, then $\lim_{t\to\infty} C(q_{s2}(t)) = x_s(0) + \delta_x - 1 = C(q_{s2}(0)) + \delta_x$ as shown in Fig.2(b). On the other hand, if $K_x \ll K_y$, then $\lim_{t\to\infty} S(q_{s2}(t)) = y_s(0) + \delta_y = S(q_{s2}(0)) + \delta_y$ as shown in Fig.2(c). The reflecting force F_R can be calculated as

$$\boldsymbol{F}_R = \left\{ \begin{array}{c} \begin{bmatrix} 0 & K_y\{S(q_{s2}(\infty)) - S(q_{s2}(0)) - \delta_y\} \end{bmatrix}^T, \\ \text{when } K_x \gg K_y, \text{ and} \\ \begin{bmatrix} K_x\{C(q_{s2}(\infty)) - C(q_{s2}(0)) - \delta_x\} & 0 \end{bmatrix}^T, \\ \text{when } K_x \ll K_y. \end{array} \right\}$$

If we see the pose of the slave manipulator and desired pose in Fig.2(a), the motion is constrained in the direction of $\pm \left[C(q_{s2}), S(q_{s2})\right]^T$, i.e., 45° direction in the above example. However, as derived in Eq.(9), the direction of the reflecting force depends on the ratio of elements of control gain under task space control. Therefore, we can conclude that wrong direction of force reflection can be generated if the conventional p-p architecture is used for a multi DOF BTS without careful analysis. The following section introduces a novel concept to solve this problem.

III. Instantaneous Restriction Space

Section II shows that the conventional p-p architecture makes a serious problem to transfer accurate direction of interaction force. In this section, we introduce a novel concept, instantaneous restriction space (IRS) to solve such problems. The proposed force reflection framework using IRS has a distinguishable strategy and concept from the conventional force reflection methods. In the conventional methods, reflecting force is generated by the result of position tracking and force tracking control between a master device and a slave robot. These approaches are available only for single DOF BTS or kinematically similar BTS as explained in section II. In order to generate accurate direction of force reflection for multi-DOF kinematically dissimilar BTS, we need more consideration of restriction space.

For example, in empty space, we feel nothing. In other words, kinesthetic sensation comes from constraint of motion. Therefore, the role of master device is to create identical constraint space which is detected at the slave side not to simply follow position and force at the slave side. Then, a human operator who interacts with a master device can feel the presence of restriction space as if he is in the space at the slave side. This concepts is the main idea of the proposed force reflection framework using IRS. Following sub-sections explain the strategy to implement the proposed concept.

A. Introduction of IRS

In free motion, an n DOF manipulator has n DOF motion space and $(r-n)$ DOF constraint space in r dimensional space. Therefore, this restriction space the manipulator can not cover is caused by insufficient DOF compared to the dimension of the task space. Moreover, if the manipulator is constrained by an obstacle or link collision, the motion space gets smaller. We call the space the manipulator can reach instantaneous motion space (IMS). The complementary subspace of IMS is defined as instantaneous restriction space (IRS) [14]. IRS can be classified into two groups, IRS_G and IRS_E as follows [13].

- IRS : The complementary subspace of instantaneous motion space (IMS)
- IRS_G : IRS caused by insufficient DOF
- IRS_E : IRS caused by exogenous constraints

B. Force Refection Using IRS

In order to detect IRS, restriction space projection (RSP) matrices are introduced as

$$\boldsymbol{R}_G \;:\; \boldsymbol{x}_d \in \mathbb{R}^r \to \boldsymbol{F}_{RG} \in IRS_G \tag{9}$$

$$\boldsymbol{R}_E \;:\; \boldsymbol{e}_q \in \mathbb{R}^n \to \boldsymbol{F}_{RE} \in IRS_E \tag{10}$$

where $\boldsymbol{R}_G$ and $\boldsymbol{R}_E$ are RSP matrices to generate reflecting forces caused by IRS_G and IRS_E, respectively. $\boldsymbol{x}_d$ is desired

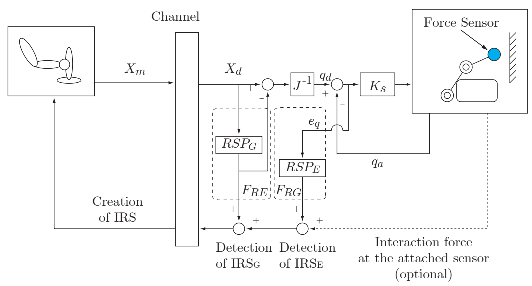

Fig. 3. Implementation of IRS in a BTS (Impedance Type)

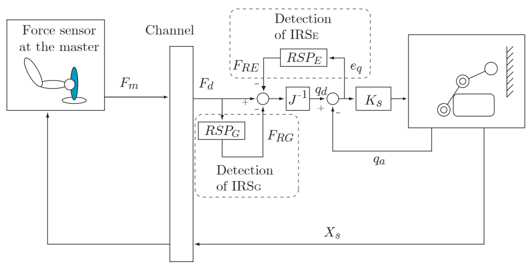

Fig. 4. Implementation of IRS in a BTS (Admittance Type)

pose. $\boldsymbol{e}_q$ is joint angle error. $\boldsymbol{F}_{RG}$ and $\boldsymbol{F}_{RE}$ are reflecting forces. $\boldsymbol{R}_G$ and $\boldsymbol{R}_E$ can be calculated as

$$\begin{aligned} \boldsymbol{R}_G &= \mathcal{C}(J)^{\perp} \in IRS_G, \text{ and} && (11) \\ \boldsymbol{R}_E &= [\{\mathcal{C}([\boldsymbol{J}_2, \boldsymbol{J}_3, \cdots, \boldsymbol{J}_n]) \oplus IRS_G\}^{\perp}, \\ & \quad \{\mathcal{C}([\boldsymbol{J}_1, \boldsymbol{J}_3, \cdots, \boldsymbol{J}_n]) \oplus IRS_G\}^{\perp}, \\ & \quad \cdots, \\ & \quad \{\mathcal{C}([\boldsymbol{J}_1, \boldsymbol{J}_2, \cdots, J_{n-1}]) \oplus IRS_G\}^{\perp}], && (12) \end{aligned}$$

where $\boldsymbol{J} = [\boldsymbol{J}_1, \boldsymbol{J}_2, \boldsymbol{J}_3 \cdots \boldsymbol{J}_n]$ and $\boldsymbol{J}_i$ is a column vector of $\boldsymbol{J}$.

From Eq.(9) and Eq.(10), RSP matrices are mappings from desired pose and error signal into reflecting forces. Therefore, the proposed algorithm is implemented to reflect force information, i.e., F_{RG} and F_{RE}, even when there is no force sensor. However, if force sensors are implemented in the interface, these sensor information can also be incorporated into our interface framework and will give more presence at the expense of expensive force sensors. Then, a general form of proposed RSP method can be implemented as shown in Fig.3.

The information from the slave side into the master side is force information which includes 1) F_{RG} caused by IRS_G, 2) F_{RE} caused by IRS_E, and 3) the interaction force sensed by force sensors at the slave manipulator if possible. This architecture is comparable to the impedance two-port interface in the sense of data flow. Fortunately, a number of results for performance and stability analysis of two-port haptic display methods in linear and passive environment in literature can be applied with the same manner to the proposed RSP architecture.

Similarly, if a BTS is admittance type, the proposed method can be implemented as shown in Fig.4. F_m is force sensed by

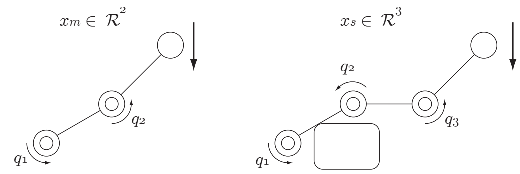

(a) Master Device (b) Slave Manipulator

Fig. 5. Case 4 in Table II

the force sensor attached at the master device. In this case, since the force command from the master side is transferred to the slave side as a desired force, $\boldsymbol{R}_G$ is defined as

$$\boldsymbol{R}_G = \mathcal{C}(J)^{\perp} \in IRS_G. \tag{13}$$

Eq.(10) to Eq.(12) can be applied to the architecture in Fig.4 in the same manner.

In section II, the wrong direction of force reflection is generated under the conventional p-p architecture. The following example shows the proposed RSP method generates accurate force reflection. In Fig.1, there is no IRS_G since a 2 DOF slave manipulator is operated in 2 dimensional task space. From Eq.(11), $\mathcal{C}(J) = R^2$ and $\boldsymbol{R}_G = \emptyset$. From Eq.(2) and Eq.12, the fact that $IRS_G \in \emptyset$, and some properties of linear algebra [15],

$$\boldsymbol{R}_E = \begin{bmatrix} C(q_{s1}+q_{s2}) & \{l_1 C(q_{s1} + l_2 C(q_{s1}+q_{s2})\}/m \\ S(q_{s1}+q_{s2}) & \{l_1 S(q_{s1} + l_2 S(q_{s1}+q_{s2})\}/m \end{bmatrix},$$

where

$$m^2 = (-l_1 S(q_1) - l_2 S(q_1+q_2))^2 + (l_1 C(q_1) + l_2 C(q_1+q_2))^2.$$

From Eq.(9), (10), $\boldsymbol{R}_G = \emptyset$, and Eq.(14), $\boldsymbol{F}_R$ can be calculated as follows.

$$\begin{aligned} \boldsymbol{F}_R &= \boldsymbol{F}_{RG} + \boldsymbol{F}_{RE} = \emptyset + \boldsymbol{R}_E \cdot \boldsymbol{e}_q \\ &= \begin{bmatrix} C(q_{s1}+q_{s2}) & \{l_1 C(q_{s1} + l_2 C(q_{s1}+q_{s2})\}/m \\ S(q_{s1}+q_{s2}) & \{l_1 S(q_{s1} + l_2 S(q_{s1}+q_{s2})\}/m \end{bmatrix} \\ &\quad \cdot \begin{bmatrix} e_{q1} \\ e_{q2} \end{bmatrix}. \end{aligned} \tag{14}$$

In Fig.1, the first joint is constrained by obstacle so that $|e_{q1}| > 0$. If we assume that $|e_{q1}| \gg |e_{q2}|$ and e_{q1} converges to zero in finite time,

$$\boldsymbol{F}_R = e_{q1} \cdot \begin{bmatrix} C(q_{s1}+q_{s2}) \\ S(q_{s1}+q_{s2}) \end{bmatrix}. \tag{15}$$

$\boldsymbol{F}_R$ generated by the proposed method has accurate direction of reflecting force.

IV. Implementation of IRS for Redundant Slave Manipulator

In Table II, case 1 to case 4 can be implemented using RSP method as shown in section III. For case 4 in TABLE II, we need more consideration. Fig.5 shows an example of the case 4 in which a slave manipulator has redundancy. If a human operator tries to move the master device (Fig.5(a)) but the slave manipulator is constrained by an obstacle (Fig.5(b)), IRS_E is detected by the RSP method. As a result, the restriction space is constructed so that the human operator feels the IRS_E, i.e., $\boldsymbol{F}_{RE}$ in Fig.3. However, it is not desirable situation since the redundancy of the slave manipulator is not used. The slave manipulator can follow the desired pose transferred from the master device even if its configuration is changed to avoid the obstacle. Since J_s has null space, there are infinite number of inverse kinematic solutions. Therefore, the problem is to choose a solution to avoid unexpected obstacles and to follow the desired pose simultaneously using detection of IRS so that a human operator commands the pose to the slave manipulator without constraints caused by the obstacle. In Fig.3, when $\boldsymbol{x}_d$ is determined, inverse kinematics solution, $\boldsymbol{q}_{sd}$, can be calculated as

$$\dot{\boldsymbol{q}}_{sd} = \boldsymbol{J}_s^{\#}\dot{\boldsymbol{x}}_d + (\boldsymbol{I}_n - \boldsymbol{J}_s^{\#}\boldsymbol{J}_s)\boldsymbol{z}, \tag{16}$$

where $\boldsymbol{I}_n$ is an identity matrix and $\boldsymbol{z}$ is an arbitrary matrix. The solution is dependant on $\boldsymbol{z}$ when $\dot{\boldsymbol{x}}_d$ and $\boldsymbol{J}_s$ are determined. In this paper, we suggest a solution

$$\dot{\boldsymbol{q}}_{sd} = \boldsymbol{J}_s^{\#}\dot{\boldsymbol{x}}_d + (\boldsymbol{I}_n - \boldsymbol{J}_s^{\#}\boldsymbol{J})(-k_1\frac{\partial p}{\partial \boldsymbol{q}_{sd}}^T - k_2\frac{\partial p}{\partial \boldsymbol{q}_{sd}}^T\frac{\partial p}{\partial \boldsymbol{q}_{sd}}\boldsymbol{J}_s^{\#}\dot{\boldsymbol{x}}_d), \tag{17}$$

where

$$\begin{aligned} p &= \frac{1}{2}\boldsymbol{e}_q^T\boldsymbol{e}_q = \frac{1}{2}(\boldsymbol{q}_{sd} - \boldsymbol{q}_s)^T(\boldsymbol{q}_{sd} - \boldsymbol{q}_s), && (18)\\ k_1 &= -k_2\dot{p} && (19)\\ k_2 &= ||\frac{\partial p}{\partial \boldsymbol{q}_{sd}}(\boldsymbol{I}_n - \boldsymbol{J}_s^{\#}\boldsymbol{J}_s)||^{-2} && (20) \end{aligned}$$

Choosing $\dot{p} < 0$, both k_1 and k_2 become positive. Unless $\frac{\partial p}{\partial \boldsymbol{q}_{sd}}(\boldsymbol{I}_n - \boldsymbol{J}_s^{\#}\boldsymbol{J}_s) = \boldsymbol{0}$, Eq.(17) guarantees the monotonous decrease of p with the specified initial velocity $\dot{p}$ as

$$\dot{p} = \frac{\partial p}{\partial \boldsymbol{q}_{sd}}\dot{q}_{sd} = -k_1\frac{\partial p}{\partial \boldsymbol{q}_{sd}}(\boldsymbol{I}_n - \boldsymbol{J}_s^{\#}\boldsymbol{J}_s)(\boldsymbol{I}_n - \boldsymbol{J}_s^{\#}\boldsymbol{J}_s)^T\frac{\partial p}{\partial \boldsymbol{q}_{sd}}^T < 0 \tag{21}$$

Therefore, $p(t) \rightarrow 0$ so that $\boldsymbol{e}_q(t) \rightarrow 0$ from Eq.(18). The physical meaning of Eq.(17) is to calculate a solution, $\dot{\boldsymbol{q}}_{sd}$ which decreases the joint angle errors so that the manipulator avoids obstacles through detection of IRS using only Jacobian, and joint angle errors without force sensor. Even if the motion of the slave manipulator is constrained by unexpected obstacles, the manipulator can follow the motion of master device minimizing reflecting force caused by the obstacles, i.e., obstacle avoidance, as far as there is redundancy of motion space.

V. EXPERIMENT

In this section, the proposed RSP method is verified through experiments for the case 4 in TABLE II explained in section IV. For a slave manipulator, 4 DOF manipulator, SOAR, the prototype of the O_2 lance manipulator for electric furnace in a steel company, POSCO [16] is used as shown in Fig.6(a). In this experiment, the third and the forth joint of SOAR are fixed and only the first and the second joint are used in order to make the problem simple. Therefore, the slave manipulator is a planar 2 DOF manipulator. The length of the first and the second link are 100mm and 100mm, respectively. The local position controller at the slave manipulator is optimized using PID tuning method developed by Choi [17]. A 1 DOF mater device in Fig.6(c) are used for the case 4.

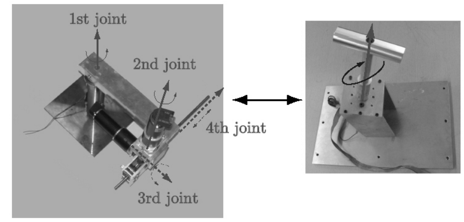

(a) (b)

Fig. 6. (a) 2 DOF slave manipulator, SOAR (b) 1 DOF master device

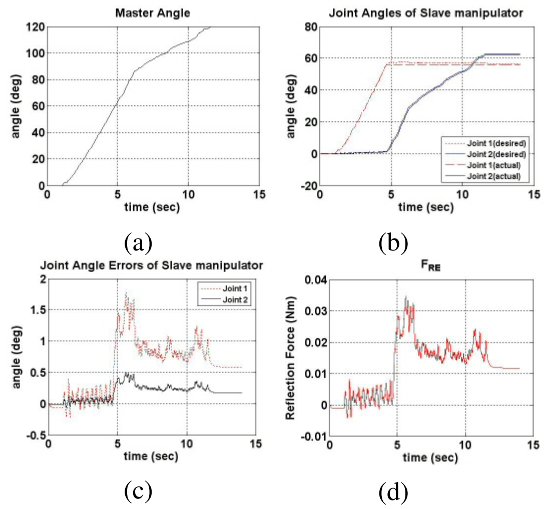

Fig. 7. (a) Master angle (b) Slave desired and actual angles (c) Joint errors of the slave manipulator (d) Reflection force

In this experiment, the proposed method for the case 4 in TABLE II, especially the method explained in section IV, is verified when the slave manipulator has redundancy. The following cases are considered.

- Exp II-1) A human operator rotates the master device in Fig.6(b) and the slave manipulator in Fig.6(a) follows the desired angle. However, at the first link, there is mechanical constraint so that the first joint is fixed at that pose.
- Exp II-2) A human operator keeps the angle of the master device in Fig.6(b). However, at the slave side, another human shakes the second link of the slave manipulator back and forth, i.e., active constraint.

If our algorithm is successfully operated, the slave manipulator should avoid the obstacle and follow the desired angle simultaneously in Exp II-1. In Exp II-2, the slave manipulator should change the joint angles to minimize the joint angle errors caused by the active constraints keeping the desired angle of the end effector. Therefore, neither reflecting force

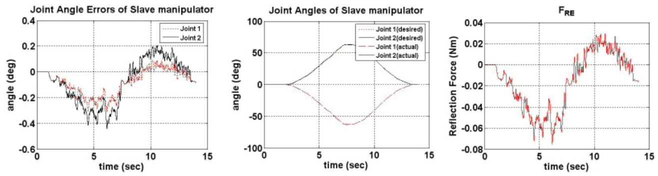

(a) (b) (c)

Fig. 8. (a) Joint errors of the slave manipulator (b) Slave desired and actual angles (c) Reflection force

nor IRS_E at the slave side are generated so that a human operator commands the motion without constraints due to the proposed algorithm using redundancy at the slave side.

Fig.7 shows the experimental result of Exp II-1. The motion of the first link is constrained by the mechanical obstacle at 4.7 second as shown in Fig.7(b). Then, the desired angles are calculated using Eq.(17) to avoid the detected obstacle. As shown in Fig.7(b), the desired angle of the first joint is calculated to maintain the angle. The error of the first joint does not increase anymore as shown in Fig.7(c). Only the second joint follows the master angle. A human operator can rotate the master device with negligible force reflection as shown in Fig.7(d).

Fig.8 shows the experimental results of Exp II-2. Fig8(a) shows joint errors caused by the active constraint. However, the slave manipulator changes the joint angles to minimize the joint angle errors maintaining the angle of the end effector of $0°$, i.e., i.e., $q_m = 0$ and $q_{s1} + q_{s2} \rightarrow 0$ as shown in Fig.8(b). Then, a human operator at the master side can keeps the angle of the master device with negligible reflecting force as shown in Fig.8(c) and the slave manipulator maintains the master angle even when active constraint changes the pose of the slave manipulator.

VI. Conclusion

It is known that the position-position (p-p) architecture is useful for a bilateral teleoperation system (BTS) when force sensors at the slave side can not detect unexpected obstacles under position-force (p-f) architecture. However, the conventional p-p architecture has limitation to generate reflecting force for kinematically dissimilar multi DOF BTSs. This limitation arises no matter which controller is used for a local controller of a kinematically dissimilar BTS (e.g. task space control and joint space control). In this paper, kinematical dissimilarity was classified into 4 cases. It was shown that the previous force reflection methods including the conventional p-p architecture can not cover all cases. Restriction space projection (RSP) method using the novel concept of instantaneous restriction space (IRS) was proposed. It was implemented for impedance type and admittance type according to the view point of data flow. Through an example, we proved that the proposed method can cover all 4 cases in TABLE II while wrong direction of force reflection is generated under the conventional p-p framework. New obstacle avoidance algorithm using redundancy of the slave manipulator was proposed for the RSP method. As a result, the proposed RSP method was applicable to case 1 to 4. Experimental results verified that the proposed method is powerful to describe the restriction space at the slave side when a BTS is kinematically dissimilar compared to the previous force reflection method. Moreover, the proposed RSP method was successfully operated in case 4 even when obstacles were active constraint caused as well as passive constraints without force sensors.

References

[1] B. Hannaford, "A design framework for teleoperators with kinesthetic feedback," *IEEE Transactions on Robotics and Automation*, vol. 5, no. 4, pp. 426–434, 1989.

[2] R. J. Anderson and M. W. Spong, "Bilateral control of teleoperators with time delay," *IEEE Transactions on Automatic Control*, vol. 34, no. 5, pp. 494–501, 1989.

[3] G. Niemeyer and J. Slotine, "Stable adaptive teleoperation," *IEEE Journal of Oceanic Engineering*, vol. 16, pp. 152–162, 1991.

[4] D. A. Lawrence, "Stability and transparency in bilateral teleoperation," *IEEE Transactions on Robotics and Automation*, vol. 9, no. 5, pp. 624–637, 1993.

[5] Y. Yokokohji and T. Yoshikawa, "Bilateral control of master-slave manipulators for ideal kinesthetic coupligng-formulation and experiment," *IEEE Transactions on Robotics and Automation*, vol. 10, no. 5, pp. 605–620, 1994.

[6] J. E. Colgate and J. M. Brown, "Factors affecting the z-width of a haptic display," in *Proceedings of the IEEE Interational Conference on Robotics and Automation*, May 1994, pp. 3205–3210.

[7] R. Oboe and P. Fiorini, "A design and control environment for internet based telerobotics," *International Journal of Robotics Research*, vol. 17, no. 4, pp. 443–449, 1998.

[8] R. J. Adams and B. Hannaford, "Stable haptic interaction with virtual environment," *IEEE Transactions on Robotics and Automation*, vol. 15, no. 3, pp. 465–474, 1999.

[9] B. Hannaford and J. H. Ryu, "Time-domain passivity control of haptic interfaces," *IEEE Transactions on Robotics and Automation*, vol. 18, no. 1, pp. 1–10, 2002.

[10] K. H. Zaad and S. E. Salcudean, "Transparency in time-delayed systems and the effect of local force feedback for transparent teleoperation," *IEEE Transaction on Robotics and Automation*, vol. 18, no. 1, pp. 109–114, 2002.

[11] M. C. Cavusoglu, A. Sherman, and F. Tendick, "Design of bilateral teleoperation controllers for haptic exploration and tele manipulation of soft environment," *IEEE Transactions on Robotics and Automation*, vol. 18, no. 4, pp. 641–647, 2002.

[12] T. Imaida, Y. Yokokohji, T. Doi, M. Oda, and T. Yoshikawa, "Ground-space bilateral teleoperation of ets-vii robot arm by direct bilateral coupling under 7-s time delay condition," *IEEE Transaction on Robotics and Automation*, vol. 20, no. 3, pp. 499–511, 2004.

[13] K. Kim, W. K. Chung, and Y. Youm, "Accurate multi-dof kinesthetic haptic display using instantaneous restriction space," in *Proc. IEEE/RSJ International Conference on Intelligent Robots and Systems*, Edmonton, Canada, Aug. 2005, pp. 716–722.

[14] D. Kim, "Kinematic analysis of spartial parallel manipulators analytic approach with the restriction space," Ph.D. dissertation, Pohang University of Science and Technology, 2001.

[15] Y. Nakamura, *Adavanced Robotics-Redundancy and Optimization*. Addison Wesley, 1991.

[16] Posco website. [Online]. Available: http://www.posco.co.kr

[17] Y. Choi, K. Yang, W. K. Chung, H. R. Kim, and I. H. Suh, "Performance and optimality of PID trajectory tracking controller for lagrangian systems," *IEEE Transactions on Robotics and Automation*, vol. 17, no. 6, pp. 857–869, 2001.